Vector field approximation using radial basis functions

Daniel A. Cervantes Cabrera, Pedro Gonzalez-Casanova, Christian Gout, L. Juárez Héctor, Rafael Resendiz

Vector field approximation using radial basis functions

Daniel A. Cervantes Cabrera

Instituto de Matemáticas, UNAM, Ciudad Universitaria, México 04510, D. F, México

Pedro González-Casanova

Instituto de Matemáticas, Ciudad Universitaria, México 04510 Mexico, D. F., México

Christian Gout

INSA Rouen, LMI, Av. de l'Université, BP 08, 76801 St Etienne du Rouvray cedex, France

L. Héctor Juárez.

Departamento de Matemáticas, Universidad Autónoma Metropolitana-Iztapalapa, Av. San Rafael Atlixco 186, Col. Vicentina, México D.F. 09340, México.

Rafael Reséndiz L.

Departamento de Matemáticas, Universidad Autónoma Metropolitana-Iztapalapa, Av. San Rafael Atlixco 186, Col. Vicentina, México D.F. 09340, México

Abstract

In this article, we investigate the performance of RBF-PDE methods to approximate solenoidal fields. It is well know that global RBF collocations methods present a trade-off principle, which means that smoothness implies high convergence order plus ill-condition. On the other hand, local methods have recently appeared in the literature to solve this problem. In this paper, we perform a numerical investigation between RBF global and local methods in order to investigate the possible advantage of local methods for the approximation of vector fields. More precisely, we compare the local Hermite interpolation technique using inverse multiquadrics versus the non symmetric collocation method of Kansa.

Keywords: Vector field approximation, radial basis functions, Runge phenomenon

1. Introduction

Radial basis functions methods have proved to be highly effective for the solution of problems both in the field of approximation theory and the solution of PDEs problems. Among other elements, this is due to their capacity of handling

complex geometries in higher dimensions for scattered nodes distributions, as well as the possibility of having spectral convergence. Due to the importance of approximating vector fields in subjects such as electromagnetism, meteorology, scientific visualization among others, we explore the possibility of these methods to solve such problems at great scale.

Despite their success, it is well known that one of the major limitations of radial basis functions (RBF) methods to solve PDEs problems is that they present high instabilities when the number of data is large or when the mesh parameter is large. This problem, known in the literature as the *uncertainty principle of Schaback* [30, 31], means that when we have exponential convergence, the corresponding condition number of the Gram matrices increases in an exponential way. Another limitation, which has recently been incorporated to this discussion, is the so called Runge phenomenon. This important limitation is implied by the fact that Gaussian RBFs interpolants in 1D, converge to a polynomial as the shape parameter tends to zero (see [11, 12, 13] for more details).

We want to mention the following methods linked to this problem for global RBFs: Fornberg et al. [14, 13] propose an expansion of the RBFs in terms of spherical harmonics, a method called QR-RBF, allow the approximation, in a stable way, of the solution for small values of the shape parameter and large number of nodes. This, however, only applies to periodical domains, such as disks or spheres, where the Runge phenomenon does not appear [12]. On the other hand, for complex domains on the plane or in space, to our knowledge, this algorithm has only been developed for non trivial node distributions [13]. However, we stress that these techniques are currently under research.

Platte and Driscoll [26] obtain node distributions making possible to calculate stable solutions for temporal problems in one dimension, or using tensor product techniques in two dimensions. They also remark that these distributions can not be obtained for problems defined on general domains and suggest to use minimum least square techniques of an over determined linear system built by using twice the number of collocation points relative to the PDEs centers.

Elsewhere, Kee, Mao and Liu [20, 22, 25, 34] use a similar approach for elasticity problems as well as inverse problems for Laplace equation by means of a local approximating scheme and node adaptive techniques. In this case, the over determination of the local systems is obtained by solving the differential equations and the boundary conditions over a set of additional nodes on the boundary.

Stevens, Power et al. [27] use a local approximating scheme, based on Hermite symmetric interpolation over local domains applied to the partial differential operator of the problem, resulting in a sparse linear system of equations for the values of the solution in each center of the local domain.

In Le Guyader et al. [16], the authors propose an alternative approach: they study a spline-based approximation of vector fields in the conservative case. In the modeling, they introduce a minimization problem on an Hilbert space: they introduce a regularized least-square problem defined on a space of potentials (real-valued functions) to fit the vector field data-set. For any $\epsilon > 0$, they

consider the functional $\mathcal{J}_\epsilon$ defined as follows:

$$\mathcal{J}_\epsilon : \begin{cases} H^{m+1}(\Omega, \mathbb{R}) \to \mathbb{R} \\ v \mapsto \langle \rho(\nabla v) - u \rangle_N^2 + \epsilon |v|_{m+1,\Omega,\mathbb{R}}^2, \end{cases}$$

where $u = (u_1, \cdots, u_N)^T \in (\mathbb{R}^n)^N$ is the vector field data-set and $|\cdot|_{m+1,\Omega,\mathbb{R}}$, the semi-norm on the Sobolev space $H^{m+1}(\Omega, \mathbb{R})$. The authors establish the existence and uniqueness of the solution, they also give convergence result in the introduced Sobolev space using norm equivalence and compactness arguments. Elsewhere, we can also mention several other approaches to study this problem: finite element approximation (see Dzhabrailov et al. [9]), PDE-based methods (see Amodei and Benbourhim [1]), spline and RBF approximations (see Awanou and Lai [2], Dodu and Rabut [7], Benbourhim and Bouhamidi [3]-[4], Ettl-Lowitsch et al. [10, 23, 24]).

Although we have emphasized the actual limitations of global RBF approximation for general domains, we stress that they are currently under intensive research and that several techniques, like domain decomposition methods [15] among others, are under way to overcome these limitations [5]. In this work, we propose local methods to get a solution of the considered vector field approximation problem. Let us note that the resulting linear system of equations is sparse.

It is important to stress that the main advantage of Steven's method is that by solving a set of small local systems of equations, a global sparse matrix is build. This makes it possible, unlike Kansa's method whose condition number can grow in an exponential way, to solve large problems. Moreover, the local systems do not increases their size as the number of nodes increases, which makes it possible to solve them in parallel. In section 4 we further investigate the running time of Stevens' algorithm for our porblem.

We recall that compactly supported RBFs methods, see Wendlad [8], which have been intensively studied, are a highly important alternative to these problems and in particular to vector field interpolation, but here we focus on RBFs spectral type convergence methods.

2. Vector field approximation: modelling

In this section, given an initial vector field u^0, which can be a prescribed function or a given set of values, we describe the mathematical formulation to approximate a vector field u as closed as possible to u^0, such that $u \cdot n = 0$ in Γ_N and $\nabla \cdot u = 0$.

We formulate the problem by means of a variational approach, which led to the solution of the corresponding Euler-Lagrange equations [17, 28]. In what follows we introduce the energy functional and the corresponding Euler Lagrange equations.

Let $\Omega \subset \mathbb{R}^d$ ($d = 2$ or 3) be an open, simply connected and bounded set with boundary $\partial\Omega = \Gamma_N \cup \Gamma_D$, where $\Gamma_N \neq \emptyset$ is the part of the boundary associated

to the surface terrain (topography), $\Gamma_D \neq \emptyset$ is the rest of the boundary and $\mathbf{n}$ is an exterior normal vector to Ω (see Figure 1).

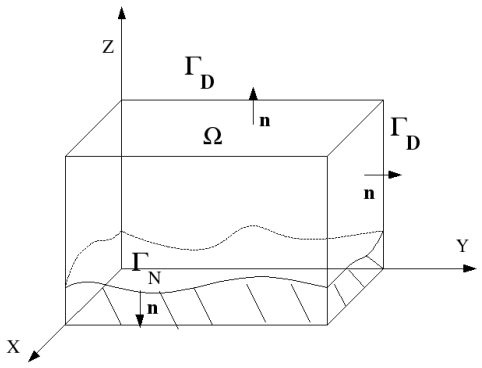

Figure 1: The studied domain Ω with boundary conditions (Neumann and Dirichlet).

So, according to the proposed method by Sasaki [29]: given an initial field u^0, the exact field of divergence free is the result of minimizing the following functional

$$\mathbf{L}(u, \lambda) = \frac{1}{2} \int_{\Omega} \{S(u - u^0) \cdot (u - u^0) + \lambda[\nabla u]\} dV$$

where λ is a Lagrange multiplier and S is a diagonal matrix related to the scales of the components of the velocity, that is

$$S = \begin{pmatrix} \alpha_1^2 & 0 & 0 \\ 0 & \alpha_2^2 & 0 \\ 0 & 0 & \alpha_3^2 \end{pmatrix}$$

where the α_i are weight parameters called Gaussian precision moduli, related to the scales of the respective components of the velocity field.

According to Ratto et al. [28] the Euler-Lagrange equations of the Lagrangian are

$$u = u^0 + S^{-1} \nabla \lambda \tag{1}$$

$$\lambda u \cdot \mathbf{n} = 0 \tag{2}$$

Finally, in [18, 17], the authors show that the Lagrange multipliers satisfy the next elliptic PDE:

$$-\nabla \cdot (S^{-1} \nabla \lambda) = \nabla \cdot u^0 \quad in \Omega, \tag{3}$$

$$\mathcal{B}_1 \lambda = g_1 \quad on \Gamma_D \tag{4}$$

$$\mathcal{B}_2 \lambda = g_2 \quad on \Gamma_N \tag{5}$$

where $\mathcal{B}_1$ and $\mathcal{B}_2$ are boundary conditions and g_1 and g_2 are given functions. Once λ is calculated, the approximated field u can be recovered from (1).

3. RBF solution

In this section, we use the classical Kansa's collocation method, with inverse multiquadric kernel $\phi(r) = (r^2 + c^2)^{-1/2}$ and we apply it on the reconstruction of a 2 dimensional solenoidal vector field u.

3.1. Non-Symmetric Collocation Method

Here, we get a radial basis approximation, so that, we can obtain the adjusted vector field u. To do that, we use Kansa's approach [19] to solve numerically the PDE system (3)-(5) for the Lagrange multiplier λ and then we obtain u from (1).

In order to do that, let us introduce the following sets of points $\Xi = \{\xi_i\}_{i=1}^N$ and $\chi = \{\mathbf{x}_i\}_{i=1}^M$ in $\mathbb{R}^d$ named *centers* and *collocations points* respectively (in this case we will take $\Xi = \chi$). Then, a radial approximation $\hat{\lambda}$ of the Lagrange multiplier λ, could be defined as follow:

$$\hat{\lambda}(\mathbf{x}) = \sum_{j=1}^{N} \beta_j \phi(r_j) = \sum_{j=1}^{N} \beta_j \phi(\|\mathbf{x} - \xi_j\|) \tag{6}$$

where $\|\mathbf{x}\| = \sqrt{x_1^2 + \cdots + x_d^2}$, $\phi : \mathbb{R}^d \to \mathbb{R}$ is the radial basis function, and the set $\{\beta\}_{j=1}^N$ are the coefficients that we must determinate.

To simplify the notations, we define the next differential operator

$$\mathcal{L} := -\nabla \cdot (S^{-1}\nabla) \tag{7}$$

Now, after substituting (6) in (3)-(5) we get

$$\sum_{j=1}^{N} \beta_j \mathcal{L}\phi(\|\mathbf{x} - \xi_j\|)|_{\mathbf{x}=\mathbf{x}_i} = \nabla \cdot u^0(\mathbf{x}_i) \quad \mathbf{x}_i \in \Omega,\ i = 1 \ldots, N_I \tag{8}$$

$$\sum_{j=1}^{N} \beta_j \mathcal{B}_1\phi(\|\mathbf{x}_i - \xi_j\|) = g_1(\mathbf{x}_i) \quad \mathbf{x}_i \in \Gamma_D,\ i = N_I + 1, \ldots, N_I + N_D \tag{9}$$

$$\sum_{j=1}^{N} \beta_j \mathcal{B}_2\phi(\|\mathbf{x} - \xi_j\|)|_{\mathbf{x}-\mathbf{x}_i} = g_2(\mathbf{x}_i) \quad \mathbf{x}_i \in \Gamma_N,\ i = N_I + N_D + 1, \ldots, N \tag{10}$$

where N_I,N_D and N_N are the number of points in Ω, Γ_D and Γ_N respectively ($N = N_I + N_D + N_N$). Equations (8)-(10), imply the algebraic system

$$A\beta = b \tag{11}$$

where the Gram matrix

$$A = \begin{bmatrix} \widetilde{A}_{\mathcal{L}} \\ \widetilde{A}_{\mathcal{B}_1} \\ \widetilde{A}_{\mathcal{B}_2} \end{bmatrix}$$

is defined as follow: for $j = 1 \ldots, N$,

$$(\widetilde{A}_{\mathcal{L}})_{i,j} = \mathcal{L}\phi(\|\mathbf{x} - \xi_j\|)|_{\mathbf{x}=x_i} \quad for i = 1, \ldots, N_I \tag{12}$$

$$(\widetilde{A}_{\mathcal{B}_1})_{i,j} = \mathcal{B}_1\phi(\|\mathbf{x}_i - \xi_j\|), \quad for i = N_I + 1, \ldots, N_I + N_D$$

$$(\widetilde{A}_{\mathcal{B}_2})_{i,j} = \mathcal{B}_2\phi(\|\mathbf{x} - \xi\|)|_{x=x_i} \; for \; i = N_I + N_D + 1, \ldots, N \tag{13}$$

To illustrate this approach, we now give an example which was studied in [17].

Example 1. *We consider the two dimensional solenoidal vector field* $\mathbf{u}(x, z) = (x, -z)$ *defined in* $\Omega = (1, 2) \times (0, 1)$. *Assuming that* $u^0(x, z) = (x, 0)$ *as an initial horizontal wind field and* $\alpha_1 = 1$, $\alpha_3 = 0.001$, *we consider the following boundary conditions in (4) and (5)*

$$\mathcal{B}_1\lambda = \lambda = g_1 = 0 \quad on\Gamma_D$$

$$\mathcal{B}_2\lambda = -S^{-1}\nabla(\lambda) \cdot \mathbf{n} = g_2 = u^0 \cdot \mathbf{n} \quad on\Gamma_N$$

In Table 1, we show the numerical results obtained with inverse multiquadric as radial basis function in (6), with different numbers of nodes and shape parameters.

Note that the condition number grows as the number of node increases or the shape parameter decreases in agreement with the uncertainty principle of Schaback [30, 31]. In order to reduce the influence of ill-conditioning in the inversion of the Gram matrix, the truncated SVD decomposition can be applied to obtain a stable solution by means of a change of basis ([32]). The results using this decomposition are displayed in Table 1. Note that the $L2$ error, for the SVD case, is good enough and that the values of the errors are reasonable when N grows or the shape parameter decreases.

c	N	$\kappa(A)$	$\nabla \cdot \hat{u}$	L2 Error
1	20	2.5e+10	2.3e-06	6.6e-01
1	60	1.1e+15	6.6e-06	7.0e-01
1	200	3.0e+23	2.0e-06	1.8e-03
0.1	20	3.1e+19	2.4e-06	4.9e-01
0.1	60	2.8e+23	1.7e-06	2.2e-05
0.1	200	4.1e+22	1.6e-06	3.7e-06
0.01	20	2.3e+19	1.7e-06	3.0e-04
0.01	60	2.7e+20	1.8e-06	2.8e-06
0.01	200	9.2e+20	1.1e-06	1.7e-06

Table 1: Inverse Gram matrix: SVD.

It is important to note that although the truncated SVD method improves our results, this algorithm can not be applied in general to large scale problems, because the technique that eliminates the singular values, simultaneously

remove their respective singular eigenvectors, degrading the basis of the space. Moreover, it should be noted that the computation of this decomposition is of order $O(2N^3)$ for square matrices, and due to this fact, some alternatives to these techniques, like domain decomposition methods or techniques based on local approximations have been developed.

In the following tables we use the notation: N number of nodes, $\kappa(A)$ number of condition the matrix A, $\nabla \cdot \hat{u}$ divergence of the approximated field $\hat{u}$ and the L2 error given by: $\frac{\|u-\hat{u}\|_2}{\|\hat{u}\|_2}$.

3.2. The Runge Phenomena

In the previous section, we noted that once the condition number is controlled, it is possible to improve the relative error when the shape parameter tends to zero, so we can expect further reducing (bounded to the machine epsilon) of this parameter, then it might be possible to obtain lower relative errors. But as shown in Table 2, this trend is preserved only for values greater than or equal to $c = 10^{-4}$ (getting a relative error of order $O(10^{-7})$), since for lower values, the relative error increases. This behavior which has been reported in [29, 12], is due to the Runge phenomena which is well known in polynomial interpolation for equidistant partitions.

c	N	$\kappa(A)$	$\nabla \cdot \hat{u}$	L2 Error
1	200	3.015e+23	2.0e-06	1.8e-03
0.1	200	4.1e+22	1.6e-06	3.7e-06
10^{-2}	200	9.2e+20	1.1e-06	1.7e-06
10^{-3}	200	1.6e+19	1.1e-06	2.2e-06
10^{-4}	200	4.5e+20	2.9e-07	6.2e-07
10^{-5}	200	4.0e+22	-3.5e-04	4.2e-04
10^{-6}	200	6.3e+24	8.3e-03	7.0e-01
10^{-7}	200	2.9e+26	8.7e-02	7.0e-01

Table 2: Runge phenomena for Kansa scheme.

The existence of the Runge phenomena for RBF approximations, was first proved by Platte and Driscoll [29], the authors prove that Gaussian kernels interpolants, for equispaced nodes in one dimension, converge to a polynomial when the shape parameter tends to zero or the number of nodes increases.

4. Local Hermitian Interpolation Method

Due to the limitations observed for global collocation methods, i.e. the uncertainty principle of Schaback and the Runge phenomena, in this section we propose to apply the local algorithm developed by Stevens, Power et al. [27] to the reconstruction of solenoidal fields. We aim to show that unlike Kansa's technique, the condition number of the global matrix corresponding to the Local Hermitian Interpolation (LHI) method does not increases in an exponential way as the number of nodes and or the shape parameter increases. In what follows

we formulate the LHI method for the vector field problem and discuss whether or not it is capable of attaining exponential order of convergence. That is, we want to study if it is competitive with respect to the global collocation method of Kansa. We shall do this by means of different numerical examples.

In this approach, the analytic solution u of a PDE system

$$\mathcal{L}u(x) = f(x) \in \Omega \tag{14}$$
$$\mathcal{B}u(x) = g(x) \in \partial\Omega \tag{15}$$

is approximated in a set of nodes $\Omega_{sc} = \{x_1, \ldots, x_{N_{sc}}\} \subset \Omega$ (called solution centers), by means of N_{sc} local sub-systems defined for each x_i as follows:

$$u(x_i) = h_i \quad x_i \in \Omega_{sc} \tag{16}$$
$$\mathcal{L}u(x) = f(x) \quad x \in \Omega_{pdec} \tag{17}$$
$$\mathcal{B}u(x) = g(x) \quad x \in \partial\Omega_{fc} \tag{18}$$

where h_i are the unknown parameters, $\Omega_{pdec} = \{x_1, \ldots, x_{N_{pdec}}\} \subset \Omega$ is a set of interior nodes related to the differential operator $\mathcal{L}$ and $\partial\Omega_{fc} = \{x_1, \ldots, x_{N_{fc}}\} \subset \partial\Omega$ the boundary nodes.

This procedure generates a set of local linear systems given by

$$A^{(k)}\beta^{(k)} = d^{(k)} \quad k = 1, \ldots, N_{sc} \tag{19}$$

which are obtained by substituting the Stevens radial Anzatz given by

$$\hat{u}^{(k)}(\mathbf{x}) = \sum_{j=1}^{N_{sc}} \beta_j^{(k)} \phi_j(r) + \sum_{j=N_{sc}+1}^{N_{sc}+N_{fc}} \beta_j^{(k)} \mathcal{B}^{\xi}\phi_j(r) +$$

$$\sum_{j=N_{sc}+N_{fc}+1}^{N_{sc}+N_{fc}+N_{pdec}} \beta_j^{(k)} \mathcal{L}^{\xi}\phi_j(r) + p_k^m \tag{20}$$

in (16)-(17), for the local domains displayed (in circles) in Figure 2. In (20), k is the local system index, N_{sc} the number of solution centers, N_{pdec} the number of PDE centers in the local system and N_{fc} the number of boundary centers in the local system. Moreover, $\mathcal{L}^{\xi}\phi_j(r) := \mathcal{L}\phi(\|\mathbf{x} - \xi\|)|_{\xi=\xi_j}$, $\mathcal{B}^{\xi}\phi_j(r) := \mathcal{B}\phi(\|\mathbf{x} - \xi\|)|_{\xi=\xi_j}$, $\phi(r)$ the inverse multiquadric and p_k^m a polynomial in $\mathbb{R}^d$ and degree m, which is defined by the null space of (14) and (15), i.e. for $d = 2$ and $m = 2$, the polynomial is given by $p(x, y) = a_0 + a_1 x + a_2 y + a_3 xy + a_4 x^2 + a_5 y^2$.

By using (19), we obtain the following Gram matrix and the right hand vector

$$A^{(k)} = \begin{bmatrix} \Phi_{ij} & \mathcal{L}^{\xi}[\Phi_{ij}] & \mathcal{B}^{\xi}[\Phi_{ij}] & P_{ij} \\ \mathcal{L}^{\mathbf{x}}[\Phi_{ij}] & \mathcal{L}^{\mathbf{x}}\mathcal{L}^{\xi}[\Phi_{ij}] & \mathcal{L}^{\mathbf{x}}\mathcal{B}^{\xi}[\Phi_{ij}] & \mathcal{L}^{\mathbf{x}}[P_{ij}] \\ \Phi_{ij} & \mathcal{L}^{\xi}[\Phi_{ij}] & \mathcal{B}^{\xi}[\Phi_{ij}] & P_{ij} \\ \mathcal{B}^{\mathbf{x}}[\Phi_{ij}] & \mathcal{B}^{\mathbf{x}}\mathcal{L}^{\xi}[\Phi_{ij}] & \mathcal{B}^{\mathbf{x}}\mathcal{B}^{\xi}[\Phi_{ij}] & \mathcal{B}^{\mathbf{x}}[P_{ij}] \end{bmatrix} \quad and \quad d^{(k)} = \begin{bmatrix} h_i \\ f_i \\ 0 \\ g_i \end{bmatrix}$$

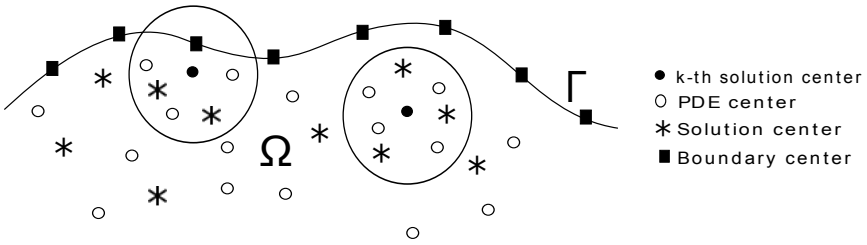

Figure 2: Centers and local subdomains for the LHI method.

Thus, each approximation $\hat{u}^{(k)}(\mathbf{x})$ has the form

$$\hat{u}^{(k)}(\mathbf{x}) = H(\mathbf{x})\beta^{(k)}(h_1, \ldots, h_{N_s}) \tag{21}$$

where

$$H^{(k)}(\mathbf{x}) = \begin{bmatrix} \phi(\|\mathbf{x}-\xi\|) & \mathcal{L}^{\xi}\phi(\|\mathbf{x}-\xi\|) & \phi(\|\mathbf{x}-\xi\|) & \mathcal{B}^{\xi}\phi(x-\xi) \end{bmatrix}$$

Finally, the local systems (19) are coupled in a global sparse linear system whose unknowns are the h_i values. This is performed by applying the differential operator $\mathcal{L}$ to each local interpolator (21) and evaluating it at the corresponding solution center, i.e.

$$\mathcal{L}[\hat{u}^{(k)}(\mathbf{x})]|_{\mathbf{x}=x_i} = f(x_i) \tag{22}$$

which is the discretization of (17). Once the values of the unknowns are obtained, the approximation of u in each solution center (see (16)) can be determined.

In our problem, i.e the approximation of vector fields, as it has been mentioned, it is necessary to calculate an approximation of the Lagrange multiplier λ by solving the corresponding Euler-Lagrange equations and by using equation (1).

It should be noted, however, that in this case it is necessary to approximate the gradient of λ, so the Stevens algorithm can not be applied directly. This is because in their case they approximate the solution, whereas in our case we need to estimate the components of the gradient of the Lagrange multiplier.

To achieve this result, we need to change the original Stevens Anzatz (20),

by incorporating the the partial derivatives in x and y in the following way

$$\hat{\lambda}_x^{(k)}(\mathbf{x}) = \sum_{j=1}^{N_{sc}} \beta_j^{(k)} \frac{\partial \phi_j(r)}{\partial x} + \sum_{j=N_{sc}+1}^{N_{sc}+N_{\mathcal{B}_1}} \beta_j^{(k)} \mathcal{B}_1^{\xi} \phi(r) + \sum_{j=N_{sc}+N_{\mathcal{B}_1}+1}^{N_{sc}+N_{\mathcal{B}_1}+N_{\mathcal{B}_2}} \beta_j^{(k)} \mathcal{B}_2^{\xi} \phi(r) + \tag{23}$$

$$+ \sum_{j=N_{sc}+N_{fc}+1}^{N_{sc}+N_{fc}+N_{pdec}} \beta_j^{(k)} \mathcal{L}^{\xi} \phi_j(r) + p^m_{\mathbf{k},\mathbf{x}}(x)$$

$$\hat{\lambda}_y^{(k)}(\mathbf{x}) = \sum_{j=1}^{N_{sc}} \beta_j^{(k)} \frac{\partial \phi_j(r)}{\partial y} + \sum_{j=N_{sc}+1}^{N_{sc}+N_{\mathcal{B}_1}} \beta_j^{(k)} \mathcal{B}_1^{\xi} \phi(r) + \sum_{j=N_{sc}+1}^{N_{sc}+N_{\mathcal{B}_2}} \beta_j^{(k)} \mathcal{B}_2^{\xi} \phi(r) \tag{24}$$

$$+ \sum_{j=N_{sc}+N_{fc}+1}^{N_{sc}+N_{fc}+N_{pdec}} \beta_j^{(k)} \mathcal{L}^{\xi} \phi_j(r) + p^m_{\mathbf{k},\mathbf{y}}(x)$$

Where $N_{\mathcal{B}_1}$ are the number of boundary nodes in Γ_D and $N_{\mathcal{B}_1}$ in Γ_N respectively and $N_{fc} = N_{\mathcal{B}_1} + N_{\mathcal{B}_2}$. The corresponding local systems are thus given by

$$\begin{cases} \frac{\partial}{\partial x}\lambda(x)|_{x=x_i} = h_i' & x_i \in \Omega_{sc} \\ \mathcal{L}\lambda(x) = f(x) & x \in \Omega_{pdec} \\ \mathcal{B}_1\lambda(x) = g_1(x) & x \in \Gamma_D \\ \mathcal{B}_2\lambda(x) = g_2(x) & x \in \Gamma_N \end{cases} \tag{25}$$

$$\begin{cases} \frac{\partial}{\partial y}\lambda(x)|_{x=x_i} = h_i'' & x_i \in \Omega_{sc} \\ \mathcal{L}\lambda(x) = f(x) & x \in \Omega_{pdec} \\ \mathcal{B}_1\lambda(x) = g_1(x) & x \in \Gamma_D \\ \mathcal{B}_2\lambda(x) = g_2(x) & x \in \Gamma_N \end{cases} \tag{26}$$

with $\mathcal{L}$ defined in (7) and $\mathcal{B}_1$ and $\mathcal{B}_2$ the boundary conditions, so that we can calculate $\nabla\lambda = (\lambda_x(x), \lambda_y(x))$. Note that $p^m_{\mathbf{k},\mathbf{x}}$ and $p^m_{\mathbf{k},\mathbf{y}}$ for our case are defined by

$$p(x,y)^2_{\mathbf{k},\mathbf{x}} = a_1 x + a_2 \frac{x^2}{2} + a_3 xy + a_4 \frac{x^2 y}{2} + a_5 \frac{x^3}{3} + a_6 xy^2 \tag{27}$$

$$p(x,y)^2_{\mathbf{k},\mathbf{y}} = \; a_1 y + a_2 xy + a_3 xy + a_3 \frac{y^2}{2} + a_5 \frac{xy^2}{3} + a_6 \frac{y^3}{3} \tag{28}$$

This is, in our opinion, a significant modification, which yields an effective methodology to compute numerical solutions of the problem, according to the results that we will show bellow. We conjecture that this type of modifications may be useful to approximate, not only the gradient, but also other type of differential operators like the rotational, when solving partial differential equations.

In order to illustrate the effectiveness of the LHI method, we display in tables (3) and (4) the CPU time of the Kansa's collocation method using SVD and the LHI method of Stevens, Power et al. ([27]) for example number 1.

We can appreciate from these tables that the CPU time (in a Intel core 2, 2.13GHz) of the LHI technique decreases at least one order of magnitude with

c	N	$\kappa(A)$	L2 Error	CPU
0.1	60	2.8e+23	2.2e-05	0.00181
0.1	200	4.1e+22	3.7e-06	0.032
0.1	400	1.4e+24	1.4e-06	0.1873
0.01	60	2.7e+20	2.8e-06	0.00175
0.01	200	9.2e+20	1.7e-06	0.0273
0.01	400	4.8e+25	5.7e-06	0.1821

Table 3: Inverse Gram matrix: SVD.

$\kappa(A)$	L2 Error	CPU
2.8e+13	2.4e-06	0.000210
2.1e+14	9.99e-03	0.00556
1.26e+14	6.85e-03	0.0171
8.1e+13	4.4e-05	0.000204
1.3e+14	2.4e-04	0.00164
2.41+14	2.5e-03	0.00663

Table 4: Inverse Global matrix: LHI.

respect to the SVD-Kansa's method. Note also that for the LHI method, a quad-tree algorith of numerical complexity $O(n\log(n))$ plus the invesion of the local matices corresponding to each solution center, must be taken into acount.

We denote A_x and A_y the global Gram matrices resulting from applying the differential operator $\mathcal{L}$ to each Anzatz (23) and (24), and evaluating them at the solution centers in agreement to equation (22). Simultaneously, A_x^{Loc} and A_y^{Loc} are the matrices which corresponds to the local systems arising form substituting (23) and (24) in equation (25) and (26) respectively.

In what follows, we shall consider first the case where the boundary conditions are of Dirichlet type and then the case where Neumann boundary conditions are taken into account. We aim to investigate whether the LHI scheme is capable to attain exponential orders of convergence, with low condition numbers for the global matrices, and if it can improve the performance of the global collocation method of Kansa. We also analyze the limitations of this method.

For this purpose, in the following numerical experiments, we display, in the first two columns of the following tables, the condition number and the $L2$ error of the global matrices. Our intention is to examine whether exponential convergence can be reached and a low condition number can be attained simultaneously. On the other hand we display, in columns four and five, the condition numbers of the local systems to analyze whether this values influence the size of the condition number of the global matrix and the $L2$ error.

Example 2. ***Approximation with Dirichlet boundary conditions.***

In this example we solve the same problem as in Example 1, but in this case we take Dirichlet boundary conditions i.e.

$$\mathcal{B}_1\lambda(\mathbf{x}) = \lambda(\mathbf{x}) = g_1(x)$$
$$\mathcal{B}_2\lambda(\mathbf{x}) = \lambda(\mathbf{x}) = g_2(x)$$

with $g_1(1,z) = g1(2,z) = \frac{\alpha_3^2}{2}(1-z^2)$, $g_1(x,1) = 0$ *and* $g_2(x,0) = \frac{\alpha_3^2}{2}$. *The results are showed in the Tables (5), (6) and Figure 3.*

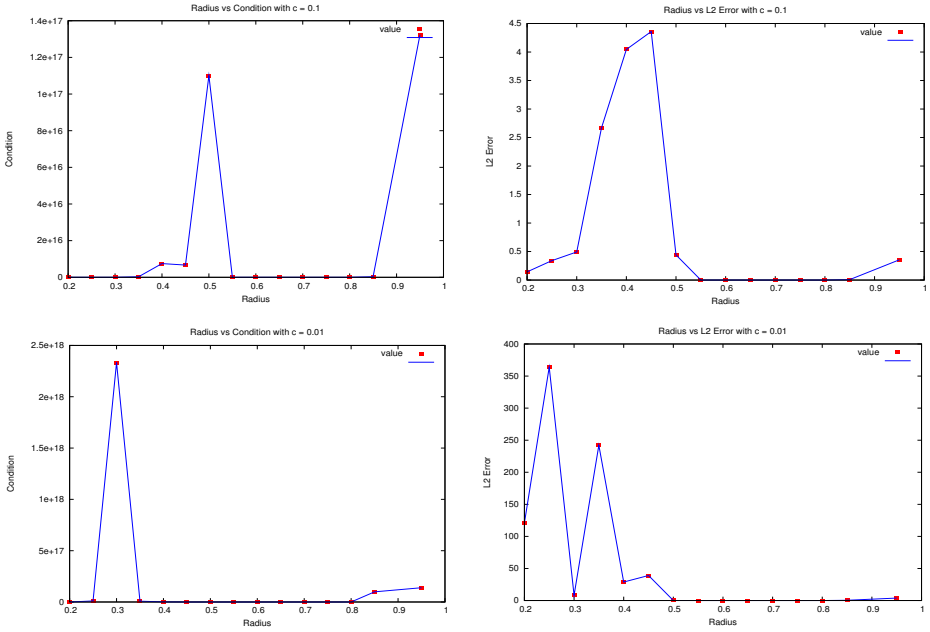

Figure 3: Top: Radius v.s. condition number and Radius v.s. L2 Error for $c = 0.1$ (table 5), Down: Radius v.s. condition number and Radius v.s. L2 Error for $c = 0.01$ (table 6).

Radius	Global $\kappa(A_y)$	$\nabla \cdot \hat{u}$	L2 Error	Max local $\kappa(A_y^{Loc})$	Min local $\kappa(A_y^{Loc})$
.2	3.8e+06	7.8e+00	1.4e-01	3.4e+27	1.2e+12
.3	1.3e+12	4.1e-02	4.9e-01	2.9e+28	1.1e+17
.4	7.4e+15	1.5e-01	4.0e+00	1.7e+29	1.0e+18
.5	1.1e+17	3.9e-03	4.4e-01	1.1e+30	1.0e+27
.6	1.9e+12	3.1e-03	2.1e-06	2.2e+30	1.6e+27
.7	5.9e+12	4.1e-03	4.2e-06	5.6e+30	1.6e+27
.8	2.7e+11	4.0e-03	3.7e-06	1.0e+30	2.6e+27
.9	1.3e+17	3.4e-03	3.5e-01	3.5e+30	4.7e+27

Table 5: LHI approximation with Dirichlet boundary conditions, number of interior nodes = 100 (50 solution centers and 50 PDE centers) and 20 boundary nodes, with shape parameter c =0.1.

Radius	Global $\kappa(A_y)$	$\nabla \cdot \hat{u}$	L2 Error	Max local $\kappa(A_y^{Loc})$	Min local $\kappa(A_y^{Loc})$
.2	7.6e+08	8.5e+02	1.2e+02	1.5e+27	2.5e+16
.3	2.3e+18	6.8e+02	8.2e+00	1.8e+27	9.1e+19
.4	1.1e+15	4.7e+01	2.8e+01	2.9e+28	3.6e+20
.5	3.7e+12	3.0e-02	1.0e-01	3.7e+27	1.7e+25
.6	1.4e+13	3.7e-03	3.1e-02	2.3e+27	3.0e+25
.7	1.4e+12	2.8e-02	3.1e-04	1.6e+27	5.3e+25
.8	3.3e+10	9.0e-02	1.3e-05	1.0e+28	4.0e+25
.9	1.3e+17	7.9e-01	3.8e+00	1.4e+27	7.2e+25

Table 6: LHI approximation with Dirichlet boundary conditions, number of interior nodes = 100 (50 solution centers and 50 PDE centers) and 20 boundary nodes, with shape parameter c =0.01.

Example 3. ***Approximation with Dirichlet-Neumann boundary conditions.***

In this example we solve the same problem as in Example 1 but this time with the same Dirichlet-Neumann boundary conditions i.e.

$$\mathcal{B}_1\lambda = \lambda = g_1 = 0 \;\; on\Gamma_D$$
$$\mathcal{B}_2\lambda = -S^{-1}\nabla(\lambda)\cdot\mathbf{n} = g_2 = u^0\cdot\mathbf{n} \;\; on\Gamma_N$$

The results are showed in the Tables (7), (8) and Figure 4.

Radius	Global $\kappa(A_y)$	$\nabla\hat{u}$	L2 Error	Max local $\kappa(A_y^{Loc})$	Min local $\kappa(A_y^{Loc})$
.2	4.6e+10	4.3e+00	3.7e+00	1.2e+22	3.8e+18
.3	1.0e+16	1.9e-01	5.4e+00	3.7e+28	3.3e+19
.4	3.6e+20	3.1e-01	5.6e-01	1.6e+29	4.9e+19
.5	3.1e+16	6.2e-01	5.4e-01	4.1e+29	8.0e+19
.6	6.8e+14	8.2e-03	1.0e-05	4.7e+30	8.1e+26
.7	3.0e+14	6.3e-03	7.7e-03	2.8e+30	1.3e+27
.8	1.6e+15	4.4e-03	1.2e-01	5.1e+29	3.7e+27
.9	2.9e+20	4.4e-01	3.1e-01	7.6e+29	4.4e+27

Table 7: LHI approximation with Dirichlet-Neumann boundary conditions, number of interior nodes = 200 (100 solution centers and 100 PDE centers) and 40 boundary nodes, with shape parameter c =0.1.

In tables (5, 6, 7 and 8) only the condition number of A_y is showed while A_x is omitted, the reason is that both values have a very similar numerical behavior.

In Tables (5) and (6) we display, for Dirichlet boundary conditions, the numerical results for two different values of the shape parameter, namely for $c = 0.1$ and $c = 0.01$. It can be observed, that the condition number of the global matrix A_y, increases with the number of nodes contained in the circle. This happen within an interval and then the condition number slows down within a region around the value 0.6. In this region it can be observed that

Radius	Global $\kappa(A_y)$	$\nabla\hat{u}$	L2 Error	Max local $\kappa(A_y^{Loc})$	Min local $\kappa(A_y^{Loc})$
.2	1.1e+14	1.5e+02	6.7e+01	1.7e+28	3.9e+16
.3	7.1e+21	2.8e-01	5.7e-01	2.0e+27	8.7e+19
.4	2.9e+21	5.9e-01	5.3e-01	1.1e+27	3.9e+20
.5	6.8e+17	1.4e-01	6.4e-01	5.5e+27	1.1e+21
.6	2.4e+14	3.6e-03	4.5e-03	1.8e+28	1.3e+25
.7	2.3e+15	1.7e-02	5.2e-03	3.3e+28	2.4e+25
.8	3.8e+12	3.4e-02	1.1e-01	1.0e+28	5.7e+25
.9	2.7e+22	4.3e-01	4.1e-01	2.7e+28	5.3e+25

Table 8: LHI approximation with Dirichlet-Neumann boundary conditions; number of interior nodes = 200 (100 solution centers and 100 PDE centers) and 40 boundary nodes, with shape parameter c =0.01.

Figure 4: Top: Radius v.s. condition number and Radius v.s. L2 Error for $c = 0.1$ (table 7), Down: Radius v.s. condition number and Radius v.s. L2 Error for $c = 0.01$ (table 8).

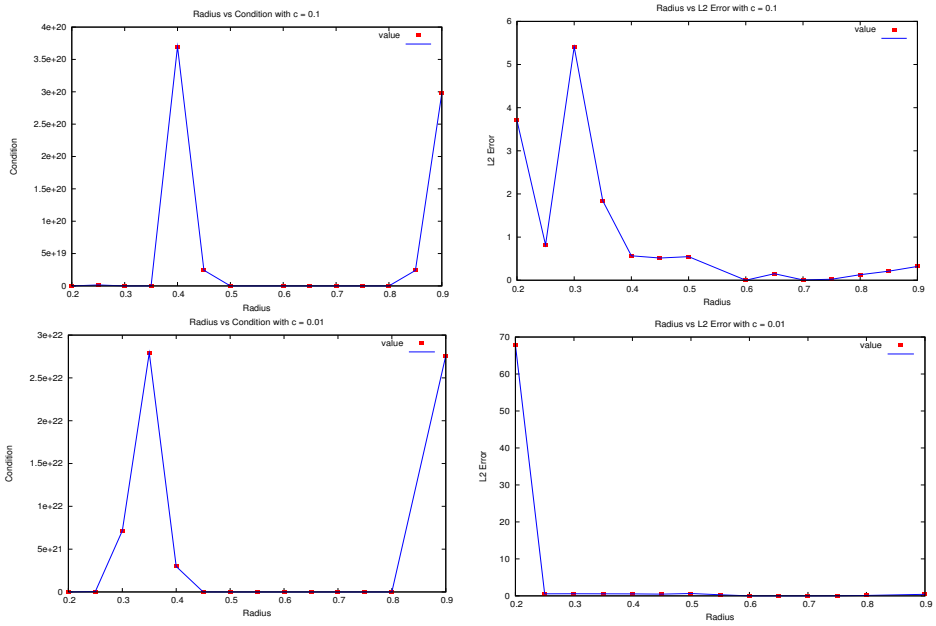

both the condition number and the error, decreases. In fact, the error is of the order of 10^{-6}, which is of the same order obtained with the global method of Kansa. These results are displayed in Figure 3. Also, it can be appreciated that the numerical approximation of the divergence is reduced within this region and its value remains constant having an order of 10^{-3}.

It can also be observed that it does not exists a direct relation between the maximum (Max local $\kappa(A_y^{Loc})$) and minimum (Min local $\kappa(A_y^{Loc})$) value of the condition number of the local matrices A_y^{Loc}.

In tables (5) and (6) we display the numerical results when the boundary conditions are of Dirichlet-Neumann type. In this case it can be observed that the behavior is similar to the Dirichlet case, the main difference is that the error is of the order of 10^{-5} instead of 10^{-6}. These results are display in Figure 4.

We stress that in both cases, Dirichlet and Dirichlet-Neumann boundary conditions, there is a region for the value for the radius, i. e. for the number of local nodes, where the approximation is nearly as good as for the global collocation method, i.e of spectral type.

5. Conclusions

In this work we have studied numerically the approximation of solenoidal vector fields. Our main objective was to compare global radial basis functions techniques, of spectral type, with local methods for inverse multiquadric kernels. Our numerical results indicate that unlike global methods, local techniques and in particular the LHI method may solve problems of great scale since the global systems of equations has a global sparse matrix with a corresponding low condition number.

The Anzatz of the LHI is flexible and it is possible to incorporate differential operators that depend to the studied problem. However, in our case, this condition was not strong enough and it was necessary to modify the Anzatz itself in order to approximate the gradient of the Lagrange multipliers. This modification of the Anzatz is a significant innovation and confirm that this technique produces good results for problems like the one considered here.

We point that in the case of Dirichlet boundary conditions, local methods achieve an error equivalent to the error obtained by the global approximation collocation techniques for this problem. The numerical experiments for vector fields were done for Cartesian meshes as well as for random data (Halton nodes) verifying that LHI scheme produced similar error in both cases. This LHI local method is highly adequate for parallel computing because the computation of the inverse of each local matrix, corresponding to each solution center, can be performed independently for multiple processors.

On the other hand, we observed that for Dirichlet-Neumann boundary conditions the LHI method produces errors which are less accurate than global collocation schemes. This agree both, with the numerical experiments performed by Stevens, Power et al. ([27]) as well as the the results for least square methods reported by Liu ([20]). In both cases the authors found that Neumann

boundary conditions produce instabilities with local methods. This behavior is a subject of current research at the scientific community.

The numerical results obtained in this work, showed that for the LHI method there is a "tread-off" principle similar to the one that exists for the compact support RBF method developed by Wendlad ([8]). More precisely, when the support of the local basis functions increases, the error of the approximated solution decreases and the condition number increases. On the other hand, if the support is small, the condition number is low but the error increases. Moreover, as it is displayed in Figures 3, 4, there is a region where the sizes of the supports of the local functions, presents small -in fact spectral- errors, and this is true for different values of the shape parameter c. Simultaneously, in this same region it can be observed, see Figure 3, that the condition number of the global matrices reaches minimum values.

Although the maximum and minimum condition number of the local basis functions are high, our results indicate that the increase of the error and the condition number of the global matrix do not depends on these values. The study of this behavior is currently a topic of our current research.

References

[1] L. Amodei and M.N. Benbourhim, *A Vector Spline Approximation*, Journal of Approximation Theory, 67(1), 51–79, 1991.

[2] G. Awanou and M. J. Lai, *Trivariate spline approximations of 3D Navier-Stokes equations*, Math. Comp., 74, 585–601, 2005.

[3] M.N. Benbourhim and A. Bouhamidi, *Approximation of vector fields by thin plate splines with tension*, Journal of Approximation Theory, 136, 198–229, 2005.

[4] M.N. Benbourhim and A. Bouhamidi, *Pseudo-polyharmonic vectorial approximation for div-curl and elastic semi-norms*, Numerische Mathematik, 109(3), 333 –364, 2008.

[5] John P. Boyd, *Six strategies for defeating the Runge Phenomenon in Gaussian radial basis functions on a finite interval*. Computers and Mathematics with Applications 60(12): 3108-3122 (2010)

[6] Chen C., Hon Y., Schaback R., *Scientific Computing with Radial Basis Functions*, Institut fur Numeriche und Angewandte Mathematik der Univesitat Gottinge, pag. 26 –33, 2003.

[7] F. Dodu and C. Rabut, *Vectorial interpolation using radial-basis-like functions*, Comput. Math. Appl., 43(3-5), 393–411, 2002.

[8] Holger Wendland, *Multiscale analysis in Sobolev spaces on bounded domains*, Numer. Math. (2010) 116:493 – 517.

[9] A.S. Dzhabrailov, Y.V. Klochkov, S.S. Marchenko and A.P. Nikolaev, *The finite element approximation of vector fields in curvilinear coordinates*, Russian Aeronautics (Iz VUZ), 50(2), 115–120, 2007.

[10] S. Ettl-Lowitzsch, J. Kaminski, M.C. Knauer, and G. Häusler, *Shape reconstruction from gradient data*, Applied Optics, 47(12), 2091–20971, 2008.

[11] B. Fornberg, G. Wright, and E. Larsson., *Some observations regarding interpolants in the limit of flat radial basis functions*, Computers and Mathematics with Applications 47 (2004) 37 – 55.

[12] Fornberg B., Zuev J., *The Runge Phenomenon and Spatially Variable Shape Parameters in RBF Interpolation*, Comput. Math. Appl. 54 (2007) 379 – 398.

[13] Fornberg B., Larsson E., Flyer N., *Stable Computations With Gaussian Radial Basis Functions*, SIAM J. on Scientific Computing 33 (2011) 869 – 892.

[14] Fornberg B., Piret C., *A Stable Algorithm for Flat Radial Basis Functions on a Sphere*, SIAM J. on Scientific Computing 30 (2007) 60 – 80.

[15] P. González-Casanova, J. Antonio Muñoz-Gómez, G. Rodríguez-Gómez, *Node Adaptive Domain Decomposition Method by Radial Basis Functions*, Journal of Numerical Methods for Partial Differential Equation , Volume 25 Issue 6, Pages 1482 - 1501, 2009.

[16] C. Le Guyader, D. Apprato and C. Gout, *Spline approximation of gradient fields: applications to wind velocity fields, in revision, MATCOM, 2012.*

[17] Flores C., Juárez H., Nuñez M., Sandoval M., *Algorithms for Vector Field Generation in Mass Consistent Models*, Numer. Methods Partial Differential Equations 26 (2010) 826 – 842. .

[18] Girault, V. and Raviart, P. A.,*Finite Element Methods for the Navier-Stokes Equations: Theory and Algorithms*, Springer-Verlag, Berlin, 1986.

[19] Kansa EJ., *Multiquadrics - a scattered data approximation scheme with applications to computational fluid dynamics II.* , Comput. Math. Appl. 19 (1990), 147 – 61.

[20] Kee B., Liu G.R., Lu C., *A least-square radial point collocation method for adaptive analysis in linear elasticity*, Engineering analysis with boundary elements 32 (2008) 440 – 460.

[21] Liu GR., Gu YT., *An introduction to meshfree methods and their programming* , Springer 2005.

[22] Liu G., Kee B., Chun Lu, *A stabilized least-squares radial point collocation method (LS-RPCM) for adaptive analysis*, Engineering analysis with boundary elements 32 (2008) 440 – 460.

[23] S. Lowitzsch, *Approximation and Interpolation employing divergence-free radial basis functions with applications*, Dissertation, Texas A&M University, 2002.

[24] S. Lowitzsch, *Error estimate for matrix-valued radial basis functions interpolation*, J. Approx. Theory, 137(2) (2005), 238–249.

[25] X.-Z. Mao, Z. Li, Least-square-based radial basis collocation method for solving inverse problems of Laplace equation from noisy data, Internat. J. Numer. Methods Engrg. 84 (2010) 1 – 26.

[29] Platte R., Driscoll T., *Polynomials and potential theory for Gaussian radial basis functions interpolation*. SIAM J. Numer. Anal. 43 (2005), 750 – 766.

[26] Platte R., Driscoll T., *Eigenvalue stability of radial basis function discretizations for time-dependent problems*, Computers Math. Applic. 51 (2006) 1251 – 1268

[27] D. Stevens, H. Power, M. Lees, H. Morvan, *A local hermitian RBF meshless numerical method for the solution of multi-zone problems*, Numerical Methods for Partial Differential Equations Volume 27, Issue 5 (2011), pages 1201 – 1230.

[28] Ratto, C.F., Festa, R.Romeo, *Mass-consisten models for wind fields over complex terrain: The estate of arte*, Eviron. Software 9 (1996), 247 – 268.

[29] Sasaki, Y., *An objective analysis based on the variational method*, Journal of the Meteorological Society of Japan 36 (1958) 77 – 88.

[30] Schaback, R., *Error estimates and condition numbers for radial basis functions interpolation*, Adv. in Comput. Math. 3 (1995), pp. 251 – 264.

[31] Schaback, R., *Multivaraite interpolation and approximation by translates of a basis funciton, in Approximation Theory*, World Scientific Publishing (Singapore), pp. 491 – 514, 1995.

[32] Schaback R., Multivariate interpolation by polynomials and radial basis functions, Constr. Approx. 21(3) (2005), 293 – 317.

[33] C. Shu, H.Ding, K.S. Yeo, *Local radial basis function-based differential quadrature method and its application to solve two-dimensional incompressible Navier-Stokes equations*, Computer Methods in Applied Mechanics and Engineering Volume 192, Issues 7-8, 14 February 2003, Pages 941 – 954.

[34] Zhang M., Xiao-Hu Liu, Kang-Zu S., Ming-Wang Lu, *Least-squares collocation meshless method*, Inter. J. Internat. J. Numer. Methods Engrg. 51 (2001) 1089 – 1100.